

This discussion paper is/has been under review for the journal Hydrology and Earth System Sciences (HESS). Please refer to the corresponding final paper in HESS if available.

# Parameterization of atmospheric long-wave emissivity in a mountainous site for all sky conditions

J. Herrero<sup>1</sup> and M. J. Polo<sup>2</sup>

<sup>1</sup>Fluvial Dynamics and Hydrology Research Group, Instituto Interuniversitario del Sistema Tierra en Andalucía, University of Granada, Spain

<sup>2</sup>Fluvial Dynamics and Hydrology Research Group, Instituto Interuniversitario del Sistema Tierra en Andalucía, Campus de Excelencia Internacional Agroalimentario ceiA3, University of Cordoba, Spain

Received: 14 February 2012 – Accepted: 11 March 2012 – Published: 21 March 2012

Correspondence to: J. Herrero (herrero@ugr.es)

Published by Copernicus Publications on behalf of the European Geosciences Union.

**HESSD**

9, 3789–3811, 2012

## Parameterization of atmospheric long-wave emissivity

J. Herrero and M. J. Polo

Title Page

Abstract

Introduction

Conclusions

References

Tables

Figures

◀

▶

◀

▶

Back

Close

Full Screen / Esc

Printer-friendly Version

Interactive Discussion



## Abstract

Long-wave radiation is an important component of the energy balance of the Earth's surface. The downward component, emitted by the clouds and aerosols in the atmosphere, is rarely measured, and is still not well understood. In mountainous areas, the models existing for its estimation through the emissivity of the atmosphere do not give good results, and worse still in the presence of clouds. In order to estimate this emissivity for any atmospheric state and in a mountainous site, we related it to the screen-level values of temperature, relative humidity and solar radiation. This permitted the obtaining of: (1) a new set of parametric equations and (2) the modification of the Brutsaert's equation for cloudy skies through the calibration of  $C$  factor to 0.34 and the parameterization of the cloud index  $N$ . Both fitted to the surface data measured at a weather station at a height of 2500 m a.s.l. in Sierra Nevada, Spain. This study analyzes separately three significant atmospheric states related to cloud cover, which were also deduced from the screen-level meteorological data. Clear and totally overcast skies are accurately represented by the new parametric expressions, while the intermediate situations corresponding to partly clouded skies, concentrate most of the dispersion in the measurements and, hence, the error in the simulation. Thus, the modeling of atmospheric emissivity is greatly improved thanks to the use of different equations for each atmospheric state.

## 1 Introduction

Long-wave radiation has an outstanding role in most of the environmental processes that take place near the Earth's surface (e.g., Philipona, 2004). Radiation exchanges at wavelengths longer than  $4\ \mu\text{m}$  between the Earth and the atmosphere above are due to the thermal emissivity of the surface and atmospheric objects, typically clouds, water vapor and carbon dioxide. This component of the radiation balance is responsible for the cooling of the Earth's surface, as it closely equals the shortwave radiation

HESSD

9, 3789–3811, 2012

## Parameterization of atmospheric long-wave emissivity

J. Herrero and M. J. Polo

Title Page

Abstract

Introduction

Conclusions

References

Tables

Figures

◀

▶

◀

▶

Back

Close

Full Screen / Esc

Printer-friendly Version

Interactive Discussion



absorbed from the sun. The modeling of the energy balance, and, hence, of the long-wave radiation balance at the surface, is necessary for many different meteorological and hydrological problems, e.g., forecast of frost and fog, estimation of heat budget from the sea (Dera, 1992), simulation of evaporation from soil and canopy, or simulation of the ice and snow cover melt (Armstrong and Brun, 2008).

Even though long-wave radiation instrumentation (pyrgeometer) is nowadays usually deployed at weather stations specifically designed for scientific purposes (e.g., Sicart et al., 2006), it is not so common in the most habitual automated weather stations. Hence, all energy balance models estimate long-wave components independently through different physical relations and parameterizations. Downward long-wave radiation is difficult to calculate with analytical methods, as they require detailed measurements of the atmospheric profiles of temperature, humidity, pressure, and the radiative properties of atmospheric constituents (Alados et al., 1986; Lhomme et al., 2007). To overcome this problem, atmospheric emissivity and temperature profile are usually parameterized from screen level values of meteorological variables. The use of near surface level data is justified since most incoming long-wave radiation comes from the lowest layers of the atmosphere (Ohmura, 2001).

It is relatively easy to create parameterizations to estimate emissivity under clear sky conditions. Several studies have compared the performance of different parameterizations over long-wave records (e.g., Sugitia and Brutsaert, 1993; Gabathuler et al., 2001) and for all cloudy sky conditions (Pluss and Omhura, 1996; Crawford and Duchon, 1999; Pirazzini et al., 2000; Kjaersgaard et al., 2007; Sedlar and Hock, 2009; Staiger and Matzarakis, 2010). But only a few of them were carried out on highland sites (Iziomon et al., 2003; Lhomme et al., 2007; Flerchinger et al., 2009). Besides, the effect of clouds and stratification on atmospheric emissivity is highly dependent on regional factors which may lead to the need for local expressions (e.g., Alados et al., 1986; Barbaro, et al., 2010).

But mountainous catchments are very sensitive areas as they are greatly exposed to meteorological conditions. Here, the surface energy balance has the greatest influence

## Parameterization of atmospheric long-wave emissivity

J. Herrero and M. J. Polo

Title Page

Abstract

Introduction

Conclusions

References

Tables

Figures



Back

Close

Full Screen / Esc

Printer-friendly Version

Interactive Discussion



on environmental processes, especially if snow is present. As existing measurements are scarce (e.g., Iziomon et al., 2003; Sicart et al., 2006), a correct parameterization of downward long-wave irradiance under all sky conditions is essential for these areas. Herrero et al. (2009) modeled the energy balance of the snowpack in Sierra Nevada Mountains (Spain), by the Mediterranean Sea. Different parameterizations for atmospheric long-wave emissivity (Brunt, 1932; König-Langlo and Augstein, 1994; Prata, 1996) were tested for clear sky periods, and although the best model performance was obtained using Brutsaert (1975) (same as Kimball et al., 1982; Kustas et al., 1994; Iziomon et al., 2003), the extension to cloudy conditions turned into a global underestimation of incoming long-wave radiation. This underestimation prevented the model from reproducing the different winter snow melting cycles typical of this Mediterranean low-latitude area. This problem was overcome through the use of a simple parameterization for atmospheric emissivity based on 2-yr screen level values of solar radiation, temperature and relative humidity that greatly improved the simulation of the snow cover evolution (Herrero et al., 2009).

In this work, a deeper analysis of long-wave incoming radiation through measurements and its relation to other meteorological data in a high mountain site is presented. From this analysis, a local parameterization for atmospheric emissivity under all sky conditions, based on 5-min surface measurements of relative humidity, temperature, and solar radiation is proposed and validated against direct local measurements. To this purpose, two different approaches were performed: (1) a new empirical expression for Sierra Nevada from 5 yr of surface meteorological data furthering the results in Herrero et al. (2009); (2) a local correction of Brutsaert's equation (Brutsaert, 1982) by means of the parameterization of its cloudiness-related index,  $N$ .

## 2 Site description and instrumentation

The study site is the southern slope of Sierra Nevada Mountain (Fig. 1), located 35 km north from the Mediterranean Sea in Southeastern Spain (37.5° N). This mountain

## Parameterization of atmospheric long-wave emissivity

J. Herrero and M. J. Polo

Title Page

Abstract

Introduction

Conclusions

References

Tables

Figures

◀

▶

◀

▶

Back

Close

Full Screen / Esc

Printer-friendly Version

Interactive Discussion



## Parameterization of atmospheric long-wave emissivity

J. Herrero and M. J. Polo

Title Page

Abstract

Introduction

Conclusions

References

Tables

Figures

◀

▶

◀

▶

Back

Close

Full Screen / Esc

Printer-friendly Version

Interactive Discussion



range raises 3500 m a.s.l. and runs parallel to the sea for approximately 60 km. It is characterized by high altitudinal gradients and a heterogeneity produced by a high mountain climate influenced by the surrounding Mediterranean climate. The presence and influence of winter snow becomes important at above 2000 m a.s.l. The snowmelt season generally extends from April to June, even though the mild winter periods characteristic of the Mediterranean climate can melt most of the snow before the end of the snow season (typically during January and February). Typically, several consecutive accumulation/melting cycles take place during one year. Sublimation from the snow can also be very important, up to 40 % of year snow precipitation, if the appropriate meteorological conditions prevail (Herrero et al., 2009).

An automatic weather station was operated in Refugio Poqueira (RP Station), at 2500 m a.s.l. (Herrero et al., 2011). Measurements of incoming shortwave and long-wave radiation (Kipp&Zonen SP-Lite pyranometer and CGR3 pyrgeometer), and 2-m air temperature and relative humidity (Vaisala HMP45), among others, have been conducted continuously since November 2005. The CGR3 pyrgeometer has a spectral range comprised between 4.5 and 44  $\mu\text{m}$  and an accuracy of 5  $\text{W m}^{-2}$ . A Campbell CR-510 datalogger recorded 5-min averages of 5 s sampling rate observations.

### 3 Data analysis

#### 3.1 Long-wave data

After the Stefan-Boltzmann Law for the radiation emission of any body at a temperature  $T$  (K), downward long-wave radiation  $L^\downarrow$  ( $\text{W m}^{-2}$ ) coming from the near-surface layer of the atmosphere may be written as:

$$L^\downarrow = \varepsilon_a \sigma T_a^4 \quad (1)$$

where  $\varepsilon_a$  is the apparent emissivity of the sky (Unsworth and Monteith, 1975),  $\sigma$  ( $\text{W m}^{-2} \text{K}^{-4}$ ) is the Stefan-Boltzmann constant, and  $T_a$  (K) is the air temperature near the surface (typically 2 m).

The downward long-wave radiation measured for 5 consecutive years at RP Station, converted to  $\varepsilon_a$  according to Eq. (1), is shown on Fig. 2a and summarized in the probability density function (pdf) in Fig. 3. The lower values of  $\varepsilon_a$  belong to clear sky situations, and in the pdf they smoothly fit a Gaussian with a mean value of 0.68 and a standard deviation of 0.0565. During very clear days, with a low temperature and relative humidity, it exhibits values ranging from 0.5 to 0.6. In the pdf, 0.77 sets the limit between clear sky and partly covered situations; higher values of  $\varepsilon_a$  denote the presence of clouds in the atmosphere. A seasonal pattern is easily observed in Fig. 2a, where the lowest emissivity values from clear skies are reached during winter. This emphasizes the importance of long-wave balance for cooling the soil and snow under high mountain clear skies. These measurements are similar to those found by Frigerio (2004) in Argentina, at 2300 m a.s.l., with night values of atmospheric emissivity under 0.7 with clear skies. Figure 2b represents daily variation of  $\varepsilon_a$ , that is, the difference between maximum and minimum daily value. It exhibits a marked seasonality, where wider daily variations of  $\varepsilon_a$  in winter are in accordance with wider variations in temperature and relative humidity. Minimum instantaneous values of  $\varepsilon_a$  during winter can be as low as 0.4, while in summer they rarely drop under 0.6.

These measured values are lower than those estimated from the usual empirical expressions, which casts a doubt over the latter for their general use in the highland under any atmospheric state. Thus, the expression by König-Langlo and Augstein (1994), used by Jordan (1999) in the SNTHERM model, gives a minimum value for emissivity of 0.765, much higher than the real values measured in this site. Prata (1996) also overestimates the lower values found under clear skies. Only Brutsaert (1975) gives more realistic values of  $\varepsilon_a$  for clear skies, and is capable to reproduce values of below 0.60 during cold days with a clear sky and low relative humidity.

## Parameterization of atmospheric long-wave emissivity

J. Herrero and M. J. Polo

Title Page

Abstract

Introduction

Conclusions

References

Tables

Figures



Back

Close

Full Screen / Esc

Printer-friendly Version

Interactive Discussion



## 3.2 Parameterizations from screen-level data

Figure 4a shows the relationship between the measured values of  $\varepsilon_a$ ,  $T_a$ , and relative humidity,  $W_a$ , for all sky conditions. In RP Station records,  $W_a$  represents the effect of the presence of water in the atmosphere better than the water vapor pressure. That relationship is especially strong for clear and completely covered skies, as shown by the low magnitudes of the standard deviation (std) in Fig. 4b for the values of  $\varepsilon_a$  under 0.7 and over 0.9, respectively. Partly covered skies appear as a transition zone between these two boundary situations. There are some differences in these relationships between daytime and night-time values, but they were not found significant for these particular data.

In order to evaluate the relationship existing between  $\varepsilon_a$  and cloudiness, the Clearness Index CI (Sugita and Brutsaert, 1993; Crawford and Duchon, 1999) has been used. CI is the ratio between the theoretical shortwave irradiance at the top of the atmosphere (extraterrestrial radiation) and the surface-measured solar radiation. By means of the CI, calculated with the topographical model described in Aguilar et al. (2010), it is possible to find out the degree of opacity of the atmosphere due to the concentration of aerosols and clouds during the hours with sunshine. Figure 5 shows how the states of clear sky (region A) and sky completely overcast (region B) are very well represented in the relation  $W_a$ -CI- $\varepsilon_a$ . The transition area between both regions concentrates the dispersion of the values (a high std). The region of the completely covered skies has a very high emissivity, of above 0.95. This means that not only there are clouds but also that they are close to the surface, which is common in mountainous areas and the reason why the relative humidity of air is highly correlated to cloudiness.

Thus, a clear sky region (A in Fig. 5a) and a completely overcast region (B in Fig. 5b) were identified from the analyses of the mean values (Fig. 5a) and their std (Fig. 5b).

## Parameterization of atmospheric long-wave emissivity

J. Herrero and M. J. Polo

Title Page

Abstract

Introduction

Conclusions

References

Tables

Figures

◀

▶

◀

▶

Back

Close

Full Screen / Esc

Printer-friendly Version

Interactive Discussion



These regions were delimited by the following expressions as a function of  $W_a$  and CI:

$$\text{Region A : } CI > 0.25 W_a^2 + 0.025 W_a + 0.65 \quad (2a)$$

$$CI < -0.25 W_a^2 - 0.625 W_a + 1.49 \quad (2b)$$

$$5 \quad \text{Region B : } CI < 2.667 W_a - 1.867 \quad (3)$$

where  $W_a$  is expressed as a fraction of one. It must be emphasized that these two regions include most of the atmospheric states found, since 59 % of all the daily states are clear skies and 14 % are completely covered skies. The intermediate states correspond to partly cloudy skies or anomalies in the two previous regions, so that it is a zone with a great dispersion in the values of  $\varepsilon_a$ .

For “clear sky” conditions, the following expression for atmospheric emissivity  $\varepsilon_a^{\text{CS}}$  was derived from a polynomial fit of the available screen-level measurements at daytime, where the non-significant terms have been neglected:

$$\varepsilon_a^{\text{CS}} = -0.8384 - 0.7086 W_a + 0.005 T_a - 0.02 W_a^2 + 0.003124 W_a T_a \quad (4)$$

15 where  $W_a$  is expressed again as a fraction of one and  $T_a$  in K. In the case of the “completely covered skies”, the emissivity  $\varepsilon_a^{\text{CCS}}$  does not show any relation to  $T_a$  but it does to CI. Therefore, the following parametric function was fitted, the variables being expressed as before:

$$\varepsilon_a^{\text{CCS}} = 1 - 1.35 CI + 1.304 W_a CI \quad (5)$$

20 For “partly covered skies”, the best fitted expression of the emissivity  $\varepsilon_a^{\text{PCS}}$  was obtained by splitting it using a threshold CI value of 0.83:

$$\varepsilon_a^{\text{PCS}} = 0.6345 + 1.128 W_a + 0.2021 CI - 1.929 W_a^2 - 0.7847 W_a CI - 0.414 CI^2 + 1.277 W_a^3 + 0.4601 W_a^2 CI + 0.3427 W_a CI^2 \quad (\text{if } CI < 0.83) \quad (6)$$

$$25 \quad \varepsilon_a^{\text{PCS}} = -0.9862 + 1.564 W_a + 1.464 CI + 0.334 W_a^2 - 1.433 W_a CI \quad (\text{if } CI \geq 0.83) \quad (7)$$

**Parameterization of atmospheric long-wave emissivity**

J. Herrero and M. J. Polo

Title Page

Abstract

Introduction

Conclusions

References

Tables

Figures

◀

▶

◀

▶

Back

Close

Full Screen / Esc

Printer-friendly Version

Interactive Discussion



In order to extend the parameterizations to the night-time data, where CI measurements are not available, their value was interpolated by taking the nearest values known using a moving average of 15 h.

Alternatively, a correction of the Brutsaert's equation extended to cloudy conditions (Eq. 8), which had proven to be the expression for emissivity that performed best at this site (Herrero et al., 2009), has been developed.

$$\varepsilon_a = \varepsilon_a^{\text{CS}} F = 1.72 (e_a/T_a)^{1/7} (1 + C N^2) \quad (8)$$

$\varepsilon_a^{\text{CS}}$  is the emissivity for clear skies,  $e_a$  is the vapor pressure near the surface in kPa, and  $F$  ( $\geq 1$ ) is the increase in the sky emissivity due to the presence of clouds. This factor is split in  $N$ , a cloud index varying between 0 for clear skies and 1 for totally overcast skies, and  $C$ , an empirical factor dependent on the cloud types. On the one hand,  $C$  was calibrated using the RP station data for completely covered skies,  $N = 1$ , with a value of 0.34 being obtained. As for  $N$ , since there are not direct measurements of cloudiness, its value has been parameterized taking the actual screen-level values of meteorological measurements into Eq. (8):

$$N = 1.18 - 0.9326 W_a + 0.577 \text{CI} + 0.7533 W_a^2 - 1.883 W_a \text{CI} - 2.708 \text{CI}^2 + 1.937 W_a^2 \text{CI} + 0.5282 W_a \text{CI}^2 + 1.853 \text{CI}^3 \quad (9)$$

Clear sky state according to Eq. (2) also applies, so, for every combination of  $W_a$  and CI in region A,  $N$  is set to 0. Similarly, the value of  $N$  obtained from Eq. (9) is never allowed to be greater than 1.

Equations (2) to (9) have been obtained from a calibration dataset composed of all the 5-min data from November, 2004, to December, 2010, including day and night-time records for any cloudiness degree. The goodness of agreement of each expression was valued by the Mean Absolute Error MAE and the Root of the Mean Square Error RMSE. Table 1 shows the agreement found for each possible combination of conditions, namely, daytime (measured CI) and night-time (interpolated CI) data, and clear/overcast skies and intermediate states.

## Parameterization of atmospheric long-wave emissivity

J. Herrero and M. J. Polo

Title Page

Abstract

Introduction

Conclusions

References

Tables

Figures

◀

▶

◀

▶

Back

Close

Full Screen / Esc

Printer-friendly Version

Interactive Discussion



## 4 Discussion

Figure 6 shows the comparison between  $\varepsilon_a$  measurements for the calibration period, and a)  $\varepsilon_a$  values estimated by the parameterized Brutsaert's expression (Eqs. 8 and 9) and b) those obtained by the new expression proposed (Eqs. 4 to 7), respectively.

Both parameterizations estimate instantaneous  $\varepsilon_a$  values with a low error. As to the sky conditions, both models adequately fit the maxima corresponding to overcast skies and the extremely low minima recorded with clear skies, with a very similar general trend (Fig. 6) but with lower error values when the new parameterization is used. The classification of the data set into 3 atmospheric states, clear, completely covered, and partly cloudy skies, allows a better adjustment of the parametric expressions. The highest error is concentrated in the intermediate atmospheric states, those with partial cloud cover, where the surface measurements are not capable of representing by themselves the complex state of the atmosphere and the presence of clouds and aerosols in it. It must be pointed out that the night-time values are well represented even though an estimated CI has been used. Brutsaert's expression performs slightly better at night-time, and it seems scarcely affected by the use of estimated instead of measured CI values.

From Fig. 6, it can be seen that the lowest values for measured  $\varepsilon_a$ , those under 0.5, are underestimated by both expressions. In fact, these measurements are taken under similar atmospheric states, corresponding to sunny winter days with low wind speeds ( $< 1 \text{ m s}^{-1}$ ), and this underestimation may be caused by the overheating of the pyrgeometer dome by solar radiation under insufficient ventilation. This effect has already been reported (e.g., Weis, 1981), but it is normally not accounted for as the induced errors are low (Lhomme et al., 2007). However, in this work the errors in measured long-wave radiation may be important for these specific meteorological conditions, with an absolute underestimation in measured  $\varepsilon_a$  up to 0.2.

A  $C$  coefficient in the extended Brutsaert's equation (Eq. 8) of below 0.34 prevents the high values of  $\varepsilon_a$ , which are measured in very cloudy states, from being reached. This is a much higher value than the 0.22 originally proposed by Brutsaert (1982). This

## Parameterization of atmospheric long-wave emissivity

J. Herrero and M. J. Polo

Title Page

Abstract

Introduction

Conclusions

References

Tables

Figures



Back

Close

Full Screen / Esc

Printer-friendly Version

Interactive Discussion



reflects the fact that, in mountainous areas, the interaction of the clouds with the surface of the terrain and, therefore, their effect on  $\varepsilon_a$  is much more intense than in valley areas. Clear sky data are well predicted in this mountainous site using the original coefficient of 1.72 in Eq. (8) suggested by Brutsaert (1975). Consequently, there was no need to correct this coefficient, as it was already pointed out by Flerchinger et al. (2009).

The proposed expressions were finally validated against the dataset during 2011, which approximately represents the 15% of the whole 5-yr dataset. The results of this validation for different atmospheric states are summarized in Table 2, where high similarity with the calibration period can be observed. The only noticeable result is the improvement in night-time predictions with Brutsaert's equation, to such a degree that the errors are clearly lower than those corresponding to daytime measurements. This fact can be explained by the unusually frequent appearance of completely covered skies at night-time during this year. Thus, errors are significantly diminished as this is the atmospheric state best simulated by this expression.

## 5 Conclusions

The long-wave measurements recorded in a weather station at an altitude of 2500 m in a Mediterranean climate are not correctly estimated by the existing models and frequently used parameterizations. These measurements show a very low atmospheric emissivity for long-wave radiation values with clear skies (up to 0.5) and a great facility for reaching the theoretical maximum value of 1 with cloudy skies. The relationships between the screen-level values of temperature, relative humidity, emissivity, and solar radiation by means of the clearness index led to the definition of different thresholds between the possible atmospheric states: clear skies, completely overcast skies, and partly cloudy skies or those in transition. For each of these states, different parametric relations between the atmospheric emissivity and these meteorological surface measurements can be defined in order to reduce uncertainty in predictions. The equation by Brutsaert (1982), which deals with two states (clear and cloudy sky) had to be

## Parameterization of atmospheric long-wave emissivity

J. Herrero and M. J. Polo

Title Page

Abstract

Introduction

Conclusions

References

Tables

Figures

◀

▶

◀

▶

Back

Close

Full Screen / Esc

Printer-friendly Version

Interactive Discussion



corrected for a proper representation of the measured data at the study site: whereas its  $C$  index had to be set to 0.34, the cloud index  $N$  could be parametrically related to the screen-level measurements of humidity and the clearness index.

Both the new 3-state parametric expressions and the Brutsaert's expression calibrated and parameterized for cloudy conditions do succeed in representing the atmospheric emissivity very effectively for any atmospheric state, even in the night-time period when the clearness index was estimated as a function of the nearest known values. As a result, it is now possible to obtain atmospheric emissivity series in stations without any long-wave direct measurements, with a direct applicability in the surroundings of Sierra Nevada. The validity of these fits is linked to their ability to characterize the state of the atmosphere, with regard to the presence of clouds, only with surface measurements of temperature, humidity, and solar radiation. Thus, although these relations are local ones, one might assume that they may be applied to other mountainous areas with a Mediterranean climate similar to that of the study site.

*Acknowledgements.* This work has been carried out within the Guadalfeo Project, funded by the Department of the Environment of the Government of Andalusia, and partially funded by the Spanish Ministry of Science and Innovation (Research Project CGL2011-25632, "Snow dynamics in Mediterranean regions and its modelling at different scales. Implications for water resource management"). M. J. Polo wants to thank G. Gómez and J. A. Polo for their valuable support.

## References

- Aguilar, C., Herrero, J., and Polo, M. J.: Topographic effects on solar radiation distribution in mountainous watersheds and their influence on reference evapotranspiration estimates at watershed scale, *Hydrol. Earth Syst. Sci.*, 14, 2479–2494, doi:10.5194/hess-14-2479-2010, 2010.
- Alados, L., Jiménez, J. I., and Castro, Y.: Thermal radiation from cloudless skies in Granada, *Theor. Appl. Climatol.*, 37, 84–89, 1986.

## Parameterization of atmospheric long-wave emissivity

J. Herrero and M. J. Polo

Title Page

Abstract

Introduction

Conclusions

References

Tables

Figures



Back

Close

Full Screen / Esc

Printer-friendly Version

Interactive Discussion



---

## Parameterization of atmospheric long-wave emissivity

J. Herrero and M. J. Polo

---

[Title Page](#)[Abstract](#)[Introduction](#)[Conclusions](#)[References](#)[Tables](#)[Figures](#)[◀](#)[▶](#)[◀](#)[▶](#)[Back](#)[Close](#)[Full Screen / Esc](#)[Printer-friendly Version](#)[Interactive Discussion](#)

- Armstrong, R. L. and Brun, E. (Eds.): Snow and Climate. Physical Processes, in: Surface Energy Exchange and Modeling, Cambridge University Press, Cambridge, 2008.
- Barbaro, E., Oliveira, A. P., Soares, J., Codato, G., Ferreira, M. J., Mlakar, P., Božnar, M. Z., and Escobedo, J. F.: Observational characterization of the downward atmospheric longwave radiation at the surface in the city of São Paulo, *J. Appl. Meteor. Climatol.*, 49, 2574–2590, doi:10.1175/2010JAMC2304.1, 2010.
- Brunt, D.: Notes on radiation in the atmosphere, *Q. J. Roy. Meteor. Soc.*, 58, 389–418, 1932.
- Brutsaert, W.: On a derivable formula for long-wave radiation from clear skies, *Water Resour. Res.*, 11, 742–744, 1975.
- Brutsaert, W.: *Evaporation into the Atmosphere*, D. Reidel Publishing Company, Dordrecht, 1982.
- Crawford, T. M. and Duchon, C. E.: An improved parameterization for estimating effective atmospheric emissivity for use in calculating daytime downwelling long-wave radiation, *J. Appl. Meteorol.*, 38, 474–480, 1999.
- Dera J.: *Marine Physics*, Elsevier, Amsterdam, 1992.
- Flerchinger, G. N., Xiao, W., Marks, D., Sauer, T. J., and Yu, Q.: Comparison of algorithms for incoming atmospheric long-wave radiation, *Water Resour. Res.*, 45, W03423, doi:10.1029/2008WR007394, 2009.
- Frigerio, E.: Radiación nocturna: campañas en Cachi, *Av. Energ. Renov. Medio Ambiente*, 8, 11.25–11.28, 2004.
- Gabathuler, M., Marty, C., and Hanselmann, K. W.: Parameterization of incoming longwave radiation in high-mountain environments, *Phys. Geogr.*, 22, 99–114, 2001.
- Herrero J., Polo, M. J., Moñino, A., and Losada, M. A.: An energy balance snowmelt model in a Mediterranean site, *J. Hydrol.*, 371, 98–107, doi:10.1016/j.jhydrol.2009.03.021, 2009.
- Herrero, J., Aguilar, C., Millares, A., Moñino, A., Polo, M. J., and Losada, M. A.: Mediterranean high mountain meteorology from continuous data obtained by a permanent meteorological station at Sierra Nevada, Spain, *EGU General Assembly, Vienna, Austria*, 3–8 April 2011, EGU2011-12893, 2011.
- Iziomon, M. G., Mayer, H., and Matzarakis, A.: Downward atmospheric irradiance under clear and cloudy skies: measurement and parameterization, *J. Atmos. Sol.-Terr. Phy.*, 65, 1107–1116, doi:10.1016/j.jastp.2003.07.007, 2003.
- Jordan, R. E., Andreas, E. L., and Makshtas, A. P.: Heat budget of snow-covered sea ice at North Pole 4, *J. Geophys. Res.*, 104, 7785–7806, doi:10.1029/1999JC900011, 1999.

## Parameterization of atmospheric long-wave emissivity

J. Herrero and M. J. Polo

Title Page

Abstract

Introduction

Conclusions

References

Tables

Figures

◀

▶

◀

▶

Back

Close

Full Screen / Esc

Printer-friendly Version

Interactive Discussion



- Kimball, B. A., Idso, S. B., and Aase, J. K.: A model for thermal radiation from partly cloudy and overcast skies, *Water Resour. Res.*, 18, 931–936, 1982.
- Kjaersgaard, J. H., Plauborg, F. L., and Hansen, S.: Comparison of models for calculating daytime long-wave irradiance using long term data set, *Agr. Forest Meteorol.*, 143, 49–63, doi:10.1016/j.agrformet.2006.11.007, 2007.
- 5 König-Langlo, G. and Augstein, E.: Parameterization of the downward long-wave radiation at the Earth's surface in polar regions, *Meteorol. Z.*, 3, 343–347, 1994.
- Kustas, W. P., Rango, A., and Uijlenhoet, R.: A simple energy budget algorithm for the snowmelt runoff model, *Water Resour. Res.*, 30, 1515–1527, 1994.
- 10 Lhomme, J.-P., Vacher, J.-J., and Rocheteau, A.: Estimating downward long-wave radiation on the Andean Altiplano, *Agric. Forest Meteorol.*, 145, 139–148, doi:10.1016/j.agrformet.2007.04.007, 2007.
- Marks, D. and Dozier, J.: A clear-sky longwave radiation model for remote alpine areas, *Theor. Appl. Climatol.*, 27, 159–187, doi:10.1007/BF02243741, 1979.
- 15 Ohmura, A.: Physical basis for the temperature-based melt-index model, *J. Appl. Meteorol.*, 40, 753–761, 2001.
- Philipona, R., Dürr, B., Marty, C., Ohmura, A., and Wild, M.: Radiative forcing – measured at Earth's surface – corroborate the increasing greenhouse effect, *Geophys. Res. Lett.*, 31, L03202, doi:10.1029/2003GL018765, 2004.
- 20 Pirazzini, R., Nardino, M., Orsini, A., Calzolari, F., Georgiadis, T., and Levizzani, V.: Parameterization of the downward longwave radiation from clear and cloudy skies at Ny Ålesund (Svalbard), in: *IRS 2000: Current Problems in Atmospheric Radiation*, 559–562, A. Deepack Publishing, Hampton, Virginia, 2000.
- Prata, A. P.: A new long-wave formula for estimating downward clear-sky radiation at the surface, *Q. J. Roy. Meteor. Soc.*, 122, 1127–1151, doi:10.1002/qj.49712253306, 1996.
- 25 Sedlar, J. and Hock, R.: Testing longwave radiation parameterizations under clear and overcast skies at Storglaciären, Sweden, *The Cryosphere*, 3, 75–84, doi:10.5194/tc-3-75-2009, 2009.
- Sicart, J. E., Pomeroy, J. W., Essery, R. L. H., and Bewley, D.: Incoming longwave radiation to melting snow: observations, sensitivity and estimation in northern environments, *Hydrol. Process.*, 20, 3697–3708, doi:10.1002/hyp.6383, 2006.
- 30 Staiger, H. and Matzarakis, A.: Evaluation of atmospheric thermal radiation algorithms for daylight hours, *Theor. Appl. Climatol.*, 102, 227–241, 2010.

- Sugita, M. and Brutsaert, W.: Cloud effect in the estimation of instantaneous downward long-wave radiation, *Water Resour. Res.*, 29, 599–605, doi:10.1029/92WR02352, 1993.
- Unsworth, M. H. and Monteith, J. L.: Long-wave radiation at the ground. I. Angular distribution of incoming radiation, *Q. J. Roy. Meteor. Soc.*, 101, 13–24, doi:10.1002/qj.49710142703, 1975.
- 5 Weiss, A.: On the performance of pyrgeometers with silicon domes, *J. Appl. Meteorol.*, 20, 962–965, 1981.

**HESSD**

9, 3789–3811, 2012

---

**Parameterization of  
atmospheric  
long-wave emissivity**

J. Herrero and M. J. Polo

---

Title Page

Abstract

Introduction

Conclusions

References

Tables

Figures

◀

▶

◀

▶

Back

Close

Full Screen / Esc

Printer-friendly Version

Interactive Discussion



## Parameterization of atmospheric long-wave emissivity

J. Herrero and M. J. Polo

Title Page

Abstract Introduction

Conclusions References

Tables Figures

◀ ▶

◀ ▶

Back Close

Full Screen / Esc

Printer-friendly Version

Interactive Discussion

**Table 1.** Summary of the goodness of agreement of Eqs. (8) and (9) (modified Brutsaert's equation) and Eqs. (4) to (7) (new 3-state parameterization) for different atmospheric states for the calibration dataset (November 2004–December 2010) as expressed by the Mean Absolute Error and the Root Mean Square Error.

Atmospheric state	Brutsaert (1982)		3-state parameterization	
	MAE	RMSE	MAE	RMSE
Daytime clear skies	0.057	0.072	0.037	0.055
Daytime covered skies	0.040	0.055	0.025	0.040
Daytime partly cloudy	0.077	0.097	0.064	0.081
Daytime all skies	0.060	0.078	0.042	0.061
Night-time all skies	0.061	0.082	0.067	0.086
All sky conditions	0.061	0.081	0.060	0.079



## Parameterization of atmospheric long-wave emissivity

J. Herrero and M. J. Polo

Title Page

Abstract Introduction

Conclusions References

Tables Figures

◀ ▶

◀ ▶

Back Close

Full Screen / Esc

Printer-friendly Version

Interactive Discussion

**Table 2.** Summary of the goodness of agreement for different atmospheric states for the validation dataset (January 2011–December 2011) as expressed by the Mean Absolute Error and the Root Mean Square Error.

Atmospheric state	Brutsaert (1982)		3-state parameterization	
	MAE	RMSE	MAE	RMSE
Daytime clear skies	0.072	0.087	0.042	0.060
Daytime covered skies	0.044	0.058	0.030	0.047
Daytime partly cloudy	0.082	0.103	0.064	0.083
Daytime all skies	0.071	0.089	0.046	0.065
Night-time all skies	0.057	0.076	0.067	0.083
All sky conditions	0.061	0.080	0.061	0.078



Discussion Paper | Discussion Paper | Discussion Paper | Discussion Paper | Discussion Paper

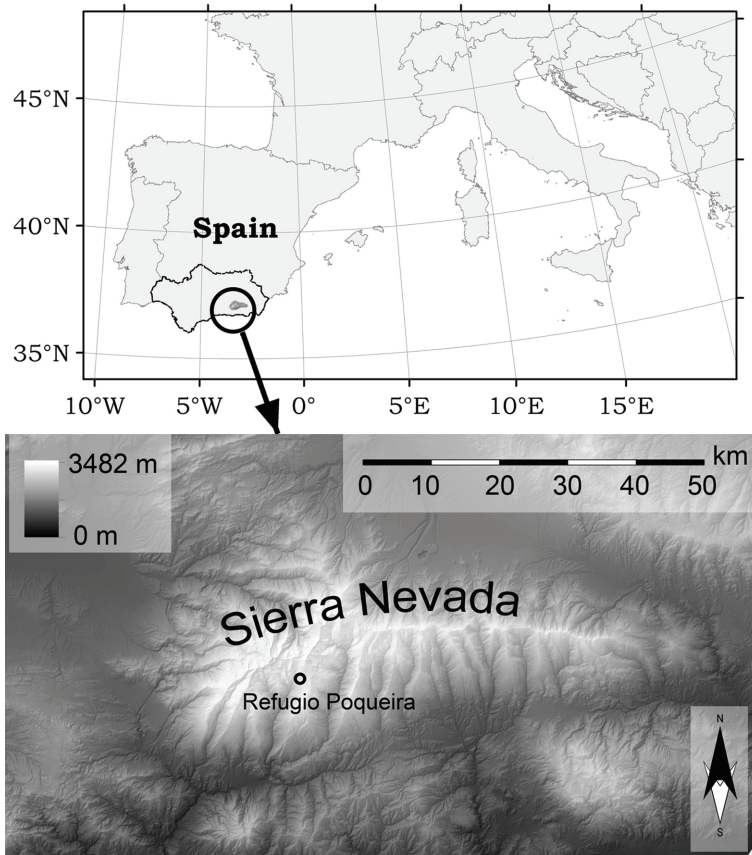


**Fig. 1.** Location of Sierra Nevada in Andalusia, Spain, and Refugio Poqueira weather station, at 2500 m a.s.l.

## Parameterization of atmospheric long-wave emissivity

J. Herrero and M. J. Polo

Title Page

Abstract

Introduction

Conclusions

References

Tables

Figures

◀

▶

◀

▶

Back

Close

Full Screen / Esc

Printer-friendly Version

Interactive Discussion



**Parameterization of  
atmospheric  
long-wave emissivity**

J. Herrero and M. J. Polo

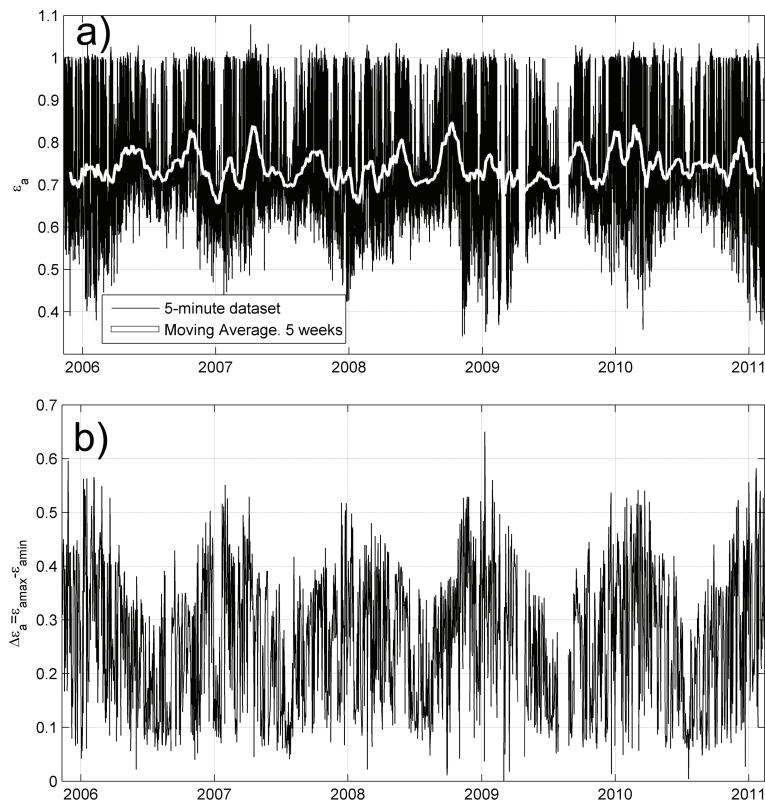


**Fig. 2.** Atmospheric emissivity measured at RP station from 2005 to 2011. **(a)** Complete dataset with 5-min frequency and the 5-weeks moving average in white. **(b)** Daily variation (difference between maximum and minimum daily values).

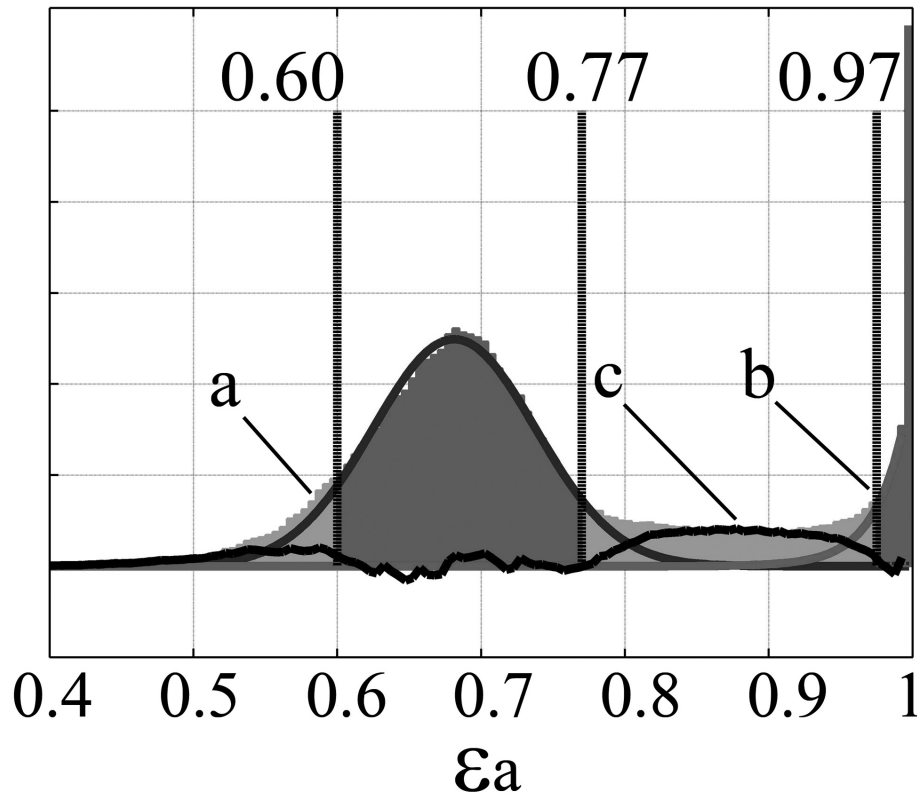


**Fig. 3.** Pdf of the atmospheric emissivity 5-min values from 2005 to 2011 with a Gaussian fit for clear sky conditions, b exponential fit for completely covered data and c residual corresponding to partly covered sky situations.

## Parameterization of atmospheric long-wave emissivity

J. Herrero and M. J. Polo

Title Page

Abstract

Introduction

Conclusions

References

Tables

Figures

◀

▶

◀

▶

Back

Close

Full Screen / Esc

Printer-friendly Version

Interactive Discussion



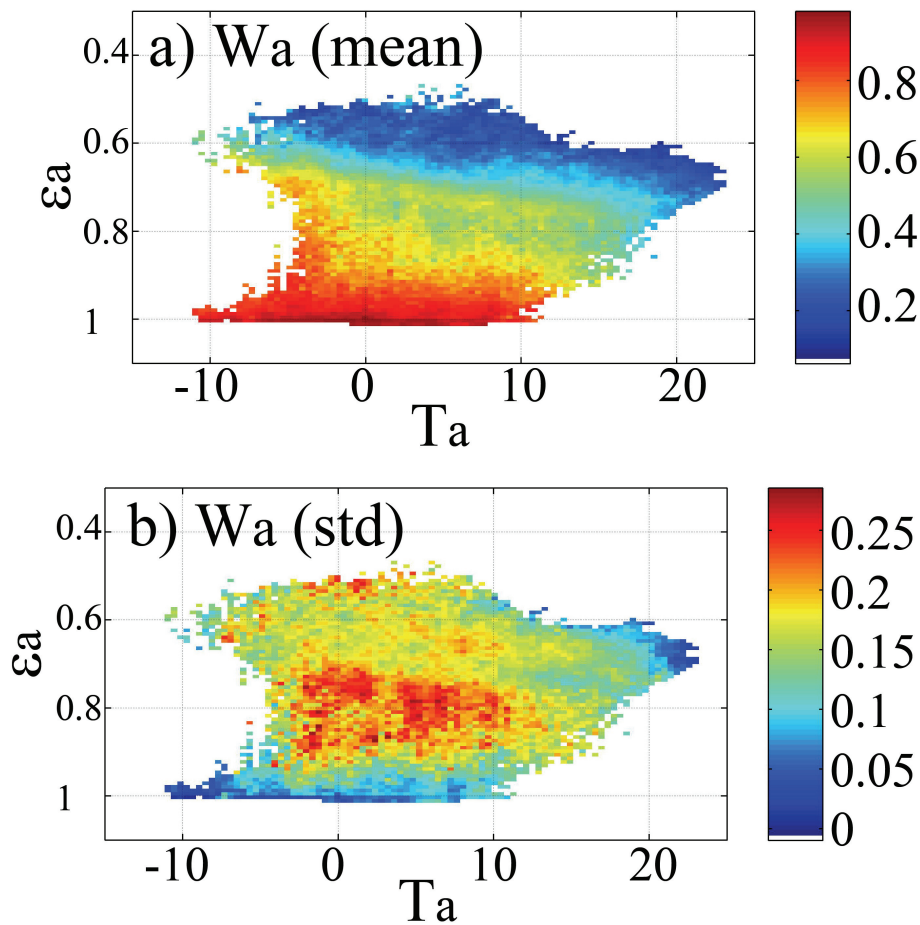


**Fig. 4.** (a) Mean value and (b) standard deviation for relative humidity  $W_a$  measurements as a function of temperature  $T_a$  and atmospheric emissivity  $\epsilon_a$ .

## Parameterization of atmospheric long-wave emissivity

J. Herrero and M. J. Polo

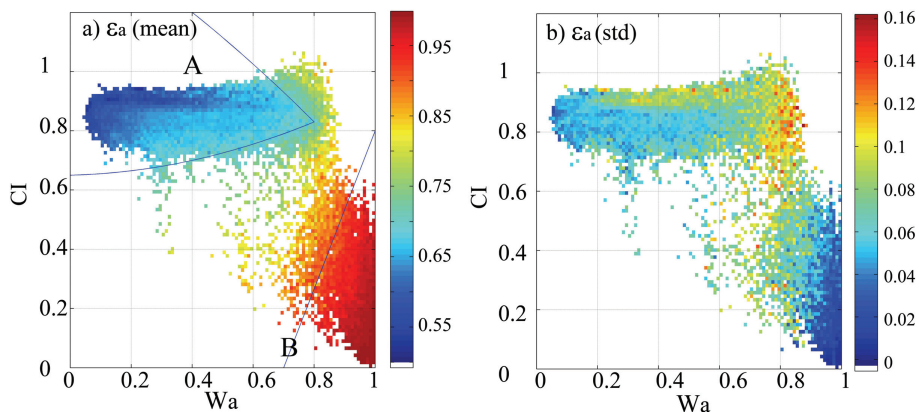


**Fig. 5.** (a) Mean value and (b) standard deviation for atmospheric emissivity measurements as a function of CI and  $W_a$ .

Title Page

Abstract

Introduction

Conclusions

References

Tables

Figures

◀

▶

◀

▶

Back

Close

Full Screen / Esc

Printer-friendly Version

Interactive Discussion



Parameterization of atmospheric long-wave emissivity

J. Herrero and M. J. Polo

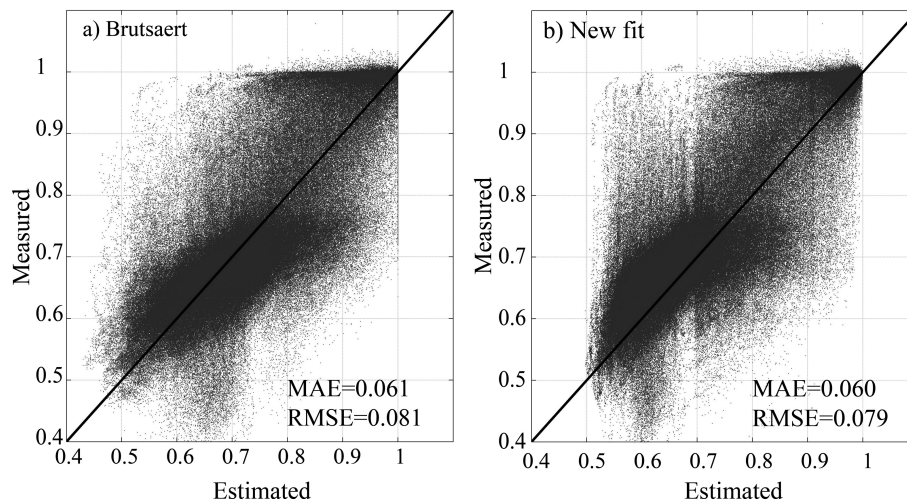


**Fig. 6.** Atmospheric emissivity measurements versus estimation using (a) Brutsaert (1982) with fitted  $N$  and (b) new parameterization.

Discussion Paper | Discussion Paper | Discussion Paper | Discussion Paper | Discussion Paper

Title Page

Abstract

Introduction

Conclusions

References

Tables

Figures

◀

▶

◀

▶

Back

Close

Full Screen / Esc

Printer-friendly Version

Interactive Discussion

